2013 IEEE International Conference on Robotics and Automation (ICRA)
Karlsruhe, Germany, May 6-10, 2013

System Identification and Control of a Small-Scale Paramotor

J. Umenberger and A. H. Göktoğan*

Abstract— **This paper presents a methodology for the system identification of a light weight, small-scale parafoil suspended motorized aircraft, known as a paramotor. The study is concerned with the acquisition of linear models describing both the lateral and longitudinal dynamics of the aircraft, with an emphasis on practical techniques that can be implemented in the real world. The mathematical models developed in this paper are first validated by comparison with real flight data, before being employed in the design of a guidance, navigation and control system, the performance of which is demonstrated by real autonomous flight tests.**

I. Introduction

A paramotor, often referred to as a powered paraglider, is a unique aircraft consisting of a ram-air inflated canopy in the shape of an aerofoil, from which a fuselage housing the propulsion system, control mechanism and other payloads is suspended. By the term small-scale we wish to emphasize that the scope of the work presented in this paper is concerned with lightweight, electric paramotors typified by the aircraft depicted in Figure 1.

Paramotors can provide a number of advantages over conventional fixed wing aircraft, including high lifting capacity, fast set-up times for rapid response launches and, when disassembled for storage, the paramotor constitutes a lightweight, compact and highly portable package [1]. These characteristics predispose the paramotor platform to military applications such as tactical reconnaissance and cargo deployment.

The literature concerning the modeling and control of ram-air inflated aircraft can be coarsely divided into two categories: 1) high fidelity studies concerned with capturing the relative motion between the canopy and the fuselage during flight, and 2) studies that model the aircraft as a single rigid body, ignoring relative motion, typically for the purpose of controller design. The former class of research has yielded a number of mathematical models in which 6 degrees of freedom (DOF) are assigned to the inertial position and orientation of the canopy, and a further 2 or 3DOF are included to allow for the relative orientation of the canopy to the fuselage. The work of [2] employed a video-measurement system to monitor relative roll, pitch and yaw between the canopy and fuselage of an unpowered, or glided, parafoil vehicle, whilst the work of [3] attached a number of inertial sensors to the parafoil canopy to identify an 8DOF model for the motorized *Buckeye* platform.

Figure 1 Small-scale paramotor in flight.

The latter class of research ignores the complex interactions between canopy and fuselage; these studies are typically focused on controller design in which simplified, linear models are preferred. There is, however, a dearth of literature concerned with the modeling, development and flight testing of complete guidance and control systems for powered paragliders, with most studies concentrating on simulating controller performance without actual flight data. The work of [4] demonstrated by experiment that model predictive control was an effective means of controlling the horizontal path of a small-scale unpowered parafoil, and conducted system identification for the lateral dynamics. In contrast, the work of [5] was concerned only with the longitudinal system identification and control of small-scale paramotors.

This paper presents a comprehensive methodology for the system identification of both the lateral and longitudinal motion of a small-scale paramotor suitable for use in the design of a guidance and control system. Linear models describing aircraft dynamics are first derived, followed by the explanation of a practical system identification methodology. The flight test validated models are then used to develop heading and altitude control systems, the performance of which is demonstrated through real autonomous flight tests.

*Research supported by the Australian Centre for Field Robotics.

J. Umenberger is with the School of Aerospace, Mechanical and Mechatronic Engineering, at The University of Sydney, NSW 2006, Australia.(e-mail: jume5347@uni.sydney.edu.au).

A. H. Göktoğan is with the Australian Centre for Field Robotics, at The University of Sydney, NSW 2006, Australia.(e-mail: a.goktogon@acfr.usyd.edu.au).

II. LATERAL DYNAMIC MODEL

A. Derivation of Model

For the purpose of system identification, it is desirable to obtain a set of linear equations that capture the underlying lateral dynamics of the system. Before proceeding with the derivation, let us clarify the mathematical notation, which has been adopted from [6]. The symbol $[a_{BC}]^D$ denotes the tensor quantity a_{BC}, measured from point 'B' w.r.t point 'C', that has been expressed or 'coordinated' as a vector in the coordinate system associated with the frame 'D', denoted $]^D$. Superscripts denote tensor quantities involving frames. $[\overline{a_{BC}}]^D$ denotes the transpose of $[a_{BC}]^D$

The derivation of the lateral dynamics model shall be accomplished by first developing a simplified 6DOF model, and then linearizing this model about a steady state of straight and level flight; all relative motion between the canopy and the fuselage shall be assumed negligible for simplicity. The geometry of such a paramotor model is depicted in Figure 2. The point 'B', located at the mass center of the aircraft, and body fixed frame $]^B$ are used to describe the position and orientation of the paramotor w.r.t the geographic frame $]^G$, which is assumed to be an inertial frame of reference. The fuselage mass center and frame, denoted 'F' and $]^F$ respectively, and parafoil mass centre and frame, denoted 'P' and $]^P$ respectively are used only to define the geometry of the vehicle.

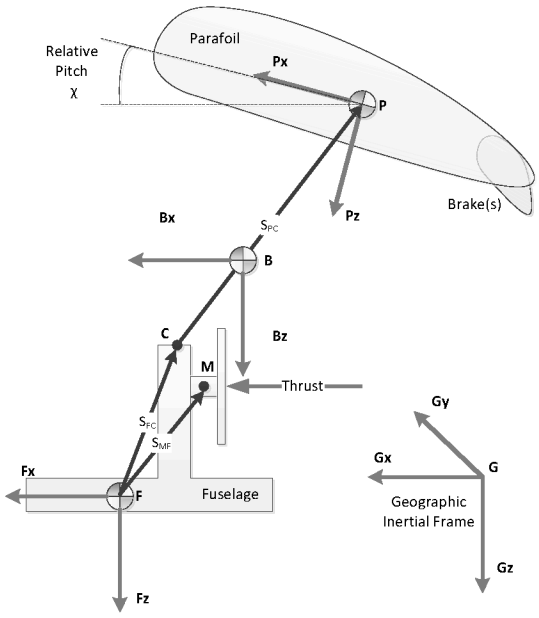

Figure 2 Paramotor coordinate system(s).

The 6DOF paramotor model consists of a 12 element state vector, including the inertial position of the mass centre in geographic frame, $[x_B^G]^G = [\overline{x, y, z}]$, the inertial velocity of the mass centre expressed in the body frame, $[v_B^G]^B = [\overline{u, v, w}]$, the rotational velocity of the body frame w.r.t the geographic frame expressed in the body frame, $[\omega^{BG}]^B = [\overline{p, q, r}]$, and the Euler angles of orientation of body frame w.r.t the geographic frame, $[\overline{\phi, \theta, \psi}]$, denoting roll, pitch and yaw. These Euler angles can be used to form the coordinate transformation matrix from geographic to the body frame,

$$[T]^{BG} = \begin{bmatrix} c_\theta c_\psi & c_\theta s_\psi & s_\theta \\ s_\phi s_\theta s_\psi - c_\phi s_\psi & s_\phi s_\theta s_\psi - c_\phi c_\psi & c_\theta s_\phi \\ c_\phi s_\theta c_\psi - s_\phi s_\psi & c_\phi s_\theta s_\psi - s_\phi c_\psi & c_\phi c_\theta \end{bmatrix} \quad (1)$$

Customary shorthand notation is employed for brevity, in which $\sin\alpha \equiv s_\alpha$, $\cos\alpha \equiv c_\alpha$ and $\tan\alpha \equiv t_\alpha$.

The translational dynamics describe the trajectory of the mass center, and are derived from Newton's second law of motion which may be formulated in the body frame as,

$$m^B \frac{d[v_B^G]^B}{dt} + m^B[\Omega^{BG}]^B[v_B^G]^B = [f]^B \quad (2)$$

The mass of the paramotor is denoted m^B, while the sum of the forces acting on the paramotor is given by f. The skew-symmetric form of the angular velocity of the paramotor relative to the geographic frame is represented by Ω^{BG}. The rotational dynamics are derived by expressing Euler's equation of motion in the body frame,

$$[I_B^B]^B \frac{d[\omega^{BG}]^B}{dt} + [\Omega^{BG}]^B[I_B^B]^B[\omega^{BG}]^B = [M_B]^B \quad (3)$$

In (3) the moment of inertia tensor of the paramotor, measured about the center of gravity, expressed in the body frame (and therefore time invariant) is denoted $[I_B^B]^B$. The sum of moments about the mass centre, expressed in the body frame is denoted $[M_B]^B$. To expedite the derivation of the lateral model, we next introduce and justify a number of simplifying assumptions.

We first assume that the moments due to the action of aerodynamic forces are negligible compared to the pure aerodynamic moments exerted upon the canopy. The work of [7] identified two contrasting steering modes, dubbed 'roll steering' and 'skid steering'. In the latter, the downward deflection of regions of the trailing edge of the parafoil, often called 'brakes', causes an increase in drag that dominates the increase in lift, thereby creating a yawing moment. This assumption effectively asserts that the skid steering mode dominates for the paramotor under consideration, which is consistent with both the findings of [7] and real flight observations. Given this assumption, the aerodynamic moments about the parafoil mass center are,

$$[M_B^A]^B = \frac{1}{2}\rho A^P {V_P}^2 \begin{bmatrix} \frac{C_{l_p} b^2 p}{2V_P} + C_{l_\phi} b\phi \\ \frac{C_{m_q} c^2 q}{2V_P} + C_{m_0} c \\ \frac{C_{n_r} b^2 r}{2V_P} \end{bmatrix} \quad (4)$$

Here we have adopted the notational convenience $\|[v_P^G]^P\| = V_P$ for brevity. The span and chord length of the parafoil are denoted b and c respectively. The air density is assumed constant and denoted ρ. The planform area for the parafoil canopy is denoted A^P. Furthermore the torque generated by asymmetric flap deflection, δ_a, is given by,

$$\left[M_\delta^A\right]^B = \frac{1}{2}\rho A^P {V_P}^2 \begin{bmatrix} \frac{C_{l_{\delta_a}} b}{d} \\ 0 \\ \frac{C_{n_{\delta_a}} b}{d} \end{bmatrix} \delta_a \tag{5}$$

The quantity d models the length of the control brake along the trailing edge of the canopy.

Secondly, we assume that the simplified equations of motion shall model deviations from a steady state of straight and level flight. Although the approximation of non-linear equations of motion about a so-called trimmed state is common practice [8] such a method is insufficient for general flight, and we should not expect adequate fidelity during aerobatic manoeuvres or a continuous turning motion. Furthermore, it is assumed that the paramotor flies at a constant forward airspeed, a phenomenon reported in the literature [5], which implies that all forces are balanced, thus eliminating (2). Finally, it is also assumed that the velocity of the mass centre is identical to the velocity of the parafoil aerodynamic center, which simplifies (3). Applying these assumptions reduces the equations of motion to,

$$[I_B^B]^B \frac{d[\omega^{BG}]^B}{dt} + [\Omega^{BG}]^B [I_B^B]^B [\omega^{BG}]^B \quad = [M_B^A]^B + \left[M_\delta^A\right]^B \tag{6}$$

Linearization is accomplished by taking the Jacobian of (5) with MATLAB's symbolic math capabilities,

$$\begin{bmatrix} \dot{\phi} \\ \dot{\psi} \\ \dot{p} \\ \dot{r} \end{bmatrix} = \rho A^P {V_P}^2 \begin{bmatrix} 0 & 0 & 1 & 0 \\ 0 & 0 & 0 & 1 \\ \frac{I_{XXI} C_{l_\phi} b}{2} & 0 & \frac{I_{XXI} C_{l_p} b^2}{4V_P} & \frac{I_{XZI} C_{n_r} b^2}{4V_P} \\ \frac{I_{ZXI} C_{l_\phi} b}{2} & 0 & \frac{I_{ZXI} C_{l_p} b^2}{4V_P} & \frac{I_{ZZI} C_{n_r} b^2}{4V_P} \end{bmatrix} \begin{bmatrix} \phi \\ \psi \\ p \\ r \end{bmatrix} + \rho A^P {V_P}^2 \begin{bmatrix} 0 \\ 0 \\ \frac{\left(I_{XXI} C_{l_{\delta_a}} b + I_{XZI} C_{n_{\delta_a}} b\right)}{2d} \\ \frac{\left(I_{ZXI} C_{l_{\delta_a}} b + I_{ZZI} C_{n_{\delta_a}} b\right)}{2d} \end{bmatrix} \delta_a \tag{7}$$

$$\left[\overline{I_B^B}\right]^B = \begin{bmatrix} I_{XXI} & I_{XYI} & I_{XZI} \\ I_{YXI} & I_{YYI} & I_{YZI} \\ I_{ZXI} & I_{ZYI} & I_{ZZI} \end{bmatrix}$$

B. System Identification of Model

The practical utility of the above model is clearly dependent on the knowledge of the five aerodynamic coefficients C_{l_ϕ}, C_{l_p}, $C_{n_r} C_{l_{\delta_a}}$ and $C_{n_{\delta_a}}$. The process of estimating these coefficients by correlating the model with actual flight data is referred to as system identification, and a recursive, weighted, least-squares approach, conducted in the time domain with a linear Kalman filter has been adopted.The states to be estimated are the coefficients, denoted $x = \left[\overline{C_{l_\phi}, C_{l_p}, C_{n_r} C_{l_{\delta_a}}, C_{n_{\delta_a}}}\right]$. As these coefficients are assumed to be time invariant, we shall ignore any process noise; as a consequence the time update equations become trivial,

$$\hat{x}_k^- = \hat{x}_{k-1}^+, \; P_k^- = P_{k-1}^+ \tag{8}$$

where P_k denotes the estimate error covariance, and the $^-$ and $^+$ superscripts denote a priori and a posteriori estimates, respectively. The measurement update equations are as follows,

$$K_k = P_k^- \overline{H} (H P_k^- \overline{H} + R)^{-1} \tag{9}$$

$$\hat{x}_k^+ = \hat{x}_k^- + K_k (z_k - H \hat{x}_k^-)$$

$$P_k^+ = (I - K_k H) P_k^-$$

where H is the linear model that maps state variables to measurable observations z_k, such that $z_k = H x_k$. R denotes the measurement noise covariance matrix which reflects the confidence in the measured observations. For the system under consideration, we re-arrange (6) as follows to obtain the H matrix,

$$\left[\dot{p_k} \quad \dot{r_k}\right] = H_k \left[\overline{C_{l_\phi}, C_{l_p}, C_{n_r} C_{l_{\delta_a}}, C_{n_{\delta_a}}}\right] \tag{10}$$

$$H_k = \rho A^P {V_P}^2 b \times \begin{bmatrix} I_{XXI}\phi_k & \frac{I_{XXI} b p_k}{2V_P} & \frac{I_{XXI}\delta_{a_k}}{d} & \frac{I_{XZI} b r_k}{2V_P} & \frac{I_{XZI}\delta_{a_k}}{d} \\ I_{ZXI}\phi_k & \frac{I_{ZXI} b p_k}{2V_P} & \frac{I_{ZXI}\delta_{a_k}}{d} & \frac{I_{ZZI} b r_k}{2V_P} & \frac{I_{ZZI}\delta_{a_k}}{d} \end{bmatrix}$$

The efficacy of the system identification methodology is demonstrated by application to actual flight data. Data was collected from the paramotor in Figure 1 which was equipped with a 3-axis accelerometer, 3-axis rate gyroscope, 3-axis magnetometer, 32bit microcontroller and 2.4 GHz radio control system. The sensor data was fused through an extended Kalman filter to provide estimates of $[\overline{\phi, \theta, \psi}]$ and $[\overline{p, q, r}]$. These estimates, along with the radio control inputs, where recorded to an on-board micro SD card during flight at a rate of 50Hz.

The 2x2 measurement error covariance matrix R used for system identification consists of the diagonal entries $R_{1,1}$ and $R_{2,2}$ which take values 0.00011 and 0.00008 respectively; these values are the sample variance of $\dot{p}$ and $\dot{r}$, based on data collected whilst the gyroscope was stationary. The off-diagonal entries are set to zero, as it is assumed there is no correlation between the white noise in p and r measurements. The estimate error covariance is initialised as a 5x5 diagonal matrix, with each diagonal entry set to 0.5. Each unknown coefficient in the state vector is initially estimated to have a value of -0.01. The measurable observations, z_k, are the time rates of change of p and r, which must be obtained by the numerical differentiation of the rates supplied by the filtered gyroscope data. The relevant physical properties of the test paramotor are summarised in Table 1.

During system identification, the paramotor was operated under manual control with asymmetrical brake deflections that resulted in minor deviation of the roll and yaw angles from the assumed straight and level reference state. The control sequence was intended to produce smooth sinusoidal roll and yaw signals that would behave well under numerical differentiation. The estimated coefficients for the state vector $\left[\overline{C_{l_\phi}, C_{l_p}, C_{n_r} C_{l_{\delta_a}}, C_{n_{\delta_a}}}\right]$ were -0.0055,-0.127,-0.0035,-0.2959 and -0.0506 respectively. The behavior of the resulting model under the same control inputs and initial conditions used for system identification was simulated in Simulink, and is compared with the measured flight data for model verification. True verification of the model requires comparison with a data set independent to that used during system identification, which is depicted in Figure 3.

III. LONGITUDINAL DYNAMIC MODEL

A. *Derivation of Model*

The longitudinal model presented below can be more accurately classified as a model of the altitude dynamics, as the only mode of longitudinal motion considered is the vertical displacement. Due to the potential difficulty of estimating lift and drag coefficients, which may require specialty equipment such as a wind tunnel or the ability to measure thrust in flight, a particularly simple mathematical model has been adopted. It is reported in the work of [5] and observed in the flight data captured during this study, that the altitude of the paramotor varies linearly with changes in thrust. Thus, we may approximate the altitude dynamics of the paramotor by,

$$\dot{z} = K_{alt}\left(f_{th} - f_{th\,0}\right) \tag{11}$$

where f_{th_0} is the throttle required for level flight, and K_{alt} is a constant. The responsiveness of the propulsion system to the throttle is modeled by a simple first order transfer function, placed in series with (11),

$$T_{motor} = \frac{\tau}{s+\tau} \tag{12}$$

The mathematical model comprised of (11) and (12) relates the altitude of the paramotor to the throttle alone; all thrust values and lift and drag coefficients have been absorbed into the constant K_{alt} and the throttle required for level flight, which considerably simplifies system identification.

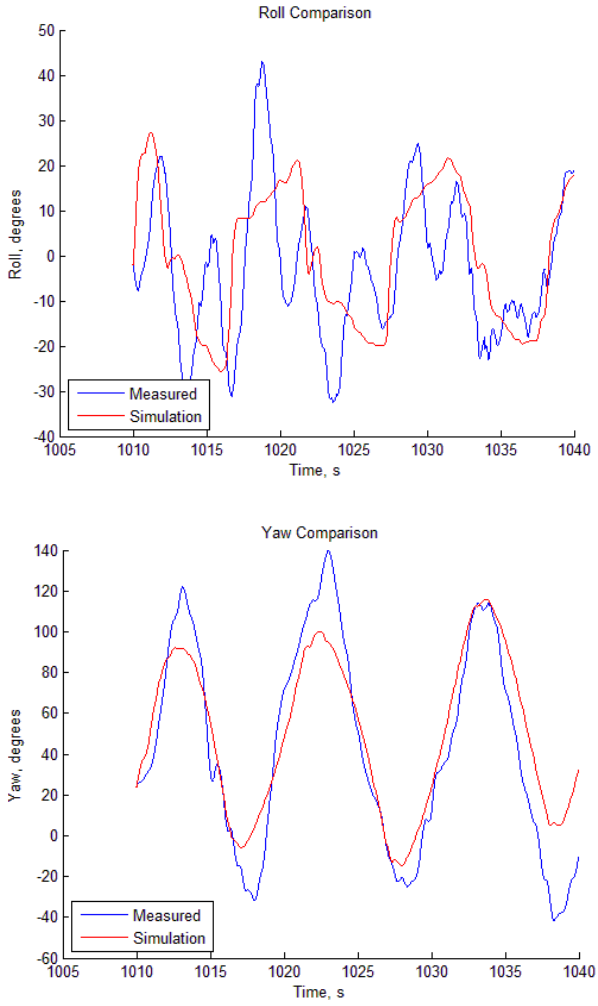

Figure 3 Measured and simulated comparison of roll and yaw.

B. *System Identification of Model*

The simplicity of the system identification method is again a reflection of the simplicity of the mathematical model, and consists of flying the paramotor under manual control at constant throttle for constant altitude, before supplying a throttle step input and measuring the subsequent rate of change of altitude, which is assumed to be constant.

The avionics package described for the system identification of the lateral model is augmented with a barometric pressure sensor, the output of which is fused with data from a Global Positioning System (GPS) receiver to estimate the altitude of the paramotor during flight.

The system identification procedure is depicted in Figure 4, which plots the normalized throttle input and the altitude over time. The throttle is held constant at 0.66 to maintain an approximately constant altitude of 54m, until a step throttle input of 0.073 is introduced at time 755s. We first note the delay in the ascending motion of the paramotor after the step increase in throttle. This delay is approximated by the rise time of the transfer function describing the transient response of the propulsion system; the time constant τ is set to 0.7 to give a rise time of 3s to a step input, by the approximation given in [9],

$$T_{rise} \approx 2.2/\tau \tag{13}$$

Linear regression is used to estimate the slope of the altitude trajectory from 758s to 762s as 16.23 m/s, which is the value of the constant K_{alt}; the units are given in m/s as the throttle input is a ratio. The performance of the resulting model is simulated in Simulink under the same initial altitude and throttle input used for system identification, and then compared with measured flight data in Figure 4.

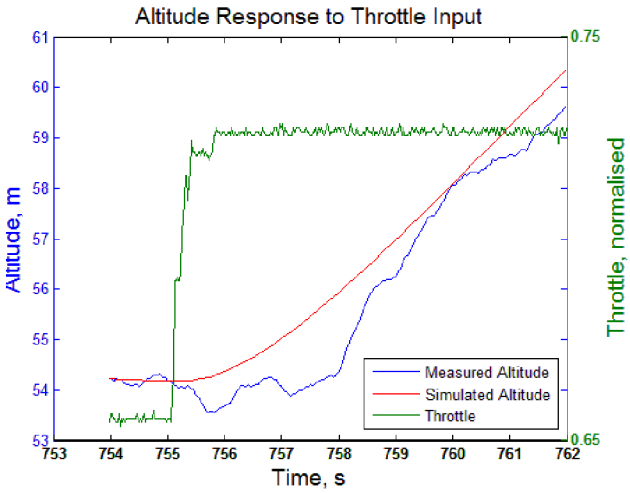

Figure 4 Measured and simulated comparison of altitude.

IV. GUIDANCE AND CONTROL

The dynamic models developed above where exploited in the development of a guidance, navigation and control system to achieve autonomous flight of the paramotor.

A. High Level Guidance Logic

The task of the high level guidance logic is to generate heading and altitude signals that will enable the paramotor to follow a desired path specified by a sequence of waypoints in inertial space. For the autonomous flight tests conducted, we are only concerned with maintaining a constant altitude; hence, the guidance logic is only concerned with the heading angle of the aircraft in the horizontal plane. The simple *look ahead* scheme implemented is depicted in Figure 5, which shows the guidance logic *looking ahead* a constant, specified distance to generate a heading angle that will direct the paramotor back to the path between the two waypoints.

B. Lateral Heading Controller

The lower-level lateral controller is effectively a heading tracking system, which receives a target heading angle from the higher-level guidance logic and outputs an asymmetric brake control signal to minimize the error between the measured and target heading. A classical feedback compensation architecture was adopted such that the angular rates output by the gyroscope could be used directly for damping. By considering the root locus of the model of the lateral dynamics developed in Section II, we were able to select the gains that achieved the desired damping ratio, which in turn was selected by nominating an arbitrary percentage overshoot and computing the damping ratio to achieve this for a second order system.

C. Longitudinal Altitude Controller

Similarly, the longitudinal controller is effectively an altitude tracking system, which receives a target altitude from the guidance scheme and outputs a throttle signal to minimize the error between the measured and target altitude. A classical proportional integral derivative (PID) controller was implemented, and again, by consulting the root locus for the model of the longitudinal dynamics of Section III we were able to select gains that achieved nominal percentage overshoot and settling time requirements for the second order system under consideration.

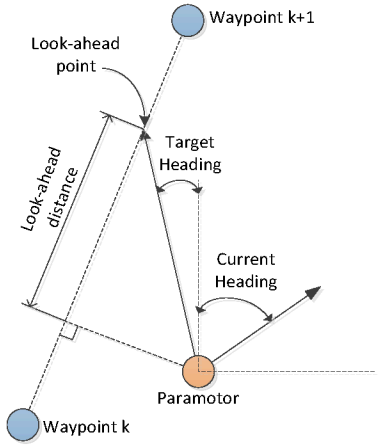

Figure 5 Look ahead guidance logic.

V. AUTONOMOUS FLIGHT TESTING

The control system described in Section IV was implemented on the aircraft of Figure 1 for verification by experimental flight testing. The aircraft was launched under manual radio control and flown to an approximate altitude of 115m above ground level in an arbitrary direction, at which point the autopilot system was engaged. The aircraft proceeded to autonomously complete a full loop of the test

circuit whilst attempting to maintain a constant altitude of 115m, as depicted in Figure 6 and Figure 7.

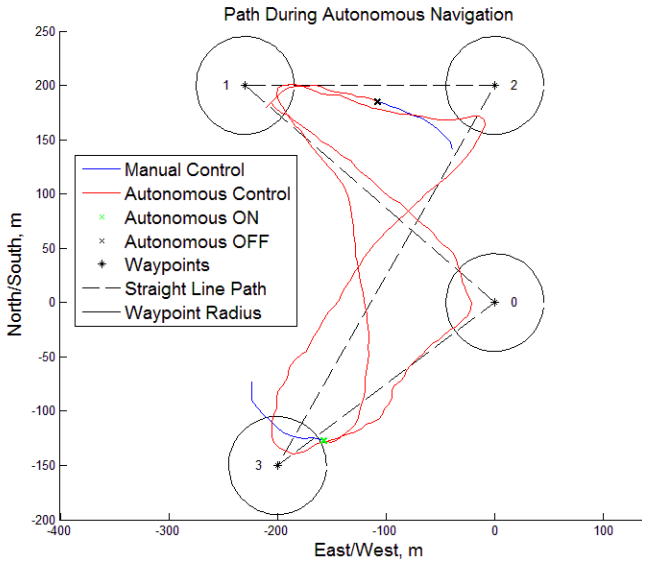

Figure 6 Horizontal path during autonomous flight.

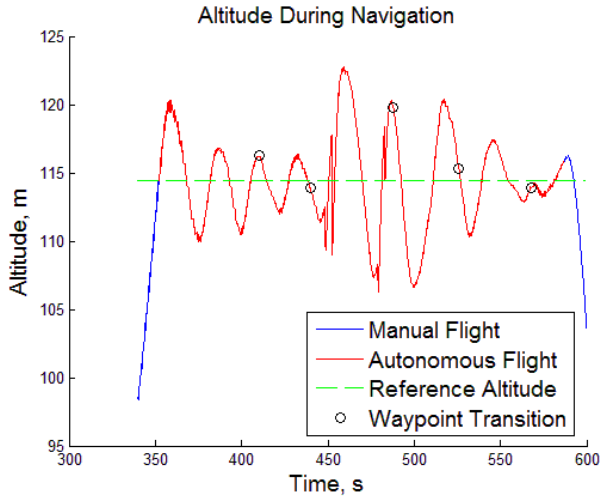

Figure 7 Altitude during autonomous flight.

VI. DISCUSSION

A. *Fidelity of Dynamic Models*

Let us begin our discussion with analysis of the fidelity of the lateral dynamic model of roll and yaw. We first observe, from Figure 3, that there is stronger agreement between simulated and measured values when considering yaw than there is when considering roll. It should be noted that for the purpose of the guidance system developed in this paper, accurate modeling of the aircraft yaw angle is more important than roll angle for inertial navigation, and so this limitation of the model is tolerated. Another consideration is the phase differences between the measured and simulated data; inspection of Figure 3 suggests that the simulated states tend to lead the measured states. This may be partially accounted for by the modeling of the control brakes as rigid flaps that can deflect instantaneously, whereas in reality, the deformation of the non-rigid trailing edge of the canopy is a complex process that will occur over a finite time.

Let us next consider the fidelity of the longitudinal dynamic model of altitude. From inspection of Figure 4 it appears that the simple longitudinal model captures the steady increase in altitude in response to a throttle step input with acceptable accuracy. It is evident, however, that first order transfer function is limited in the accuracy with which it may describe the transition between steady flight and increasing altitude, with a larger time delay observed in the measured data when compared with the simulated data.

B. *Performance of Guidance System*

Let us begin with consideration of the horizontal path following performance, where we observe that, in general, the aircraft tracks the desired path with good accuracy. This is particularly evident at the beginning of autonomous flight where the aircraft returns the *path* leading to the first waypoint, rather than merely travelling toward the waypoint from an arbitrary direction. We should note that there is some unexpected divergence from the path between waypoint 2 and waypoint 3, for which we shall attempt to account with reference to the altitude data. Turning our consideration to the performance of the altitude controller, we observe that a constant altitude is maintained within $\pm$ 7.5m of the desired value. Qualitatively, we also note the classic underdamped oscillations in altitude which demonstrates the stability of the controller, as it re-converges upon the target altitude after a disturbance. Indeed, there is considerable disturbance to the altitude at the 450s mark (Figure 7) which we attribute to wind. This disturbance also coincides with the aforementioned path divergence, and so we hypothesize that the path divergence can be attributed to both the direct action of wind upon the aircraft as well as increased variation in propeller speed as the longitudinal control system attempts to stabilize the altitude. The torque associated with these large changes in propeller angular momentum can rotate the fuselage, which can create momentary imbalances in the tension in the suspension and control lines connected to the parafoil. These imbalances can cause the aircraft to deviate from the desired path by introducing unintended yawing behavior. Finally, we wish to remark that the altitude data depicted in Figure 7 has been collected from the sensor system on board the aircraft, and so fluctuations in altitude can be attributed to sensor noise, as well as the actual motion of the aircraft. This is particularly true of the altitude estimates from the barometric pressure sensor, which is easily corrupted if exposed to direct airflow. The fact that the aircraft was capable of maintaining a stable altitude despite sensor noise and wind

disturbances, further demonstrates the stability of the system.

VII. CONCLUSION

This paper has presented a comprehensive framework for the mathematical modeling, system identification and guidance, navigation and control of a small-scale paramotor. The principle contributions of this work may be summarized as follows: a simplified 6DOF mathematical model was derived to describe the dynamics of the paramotor, which then yielded decoupled systems of linear equations for lateral and longitudinal motion. A practical system identification methodology was presented to furnish the linear models with aerodynamic coefficients, which were demonstrated to capture the underlying dynamics of the aircraft. We reported the use of well-established root locus techniques to develop a simple GNC system, the performance of which was demonstrated by autonomous flight of the paramotor along a horizontal path at constant altitude. To the best of the authors' knowledge, these results represent the first report of the successful deployment of an autonomous powered paraglider in the literature.

Table 1 List of paramotor parameters

Paramotor Physical Parameters			
Symbol	Value	Symbol	Value
m^B	1.55 kg	b	2.15 m
$[I_B^B]^B$	$\begin{bmatrix} 0.336 & 0 & -0.059 \\ 0 & 0.292 & 0 \\ -0.059 & 0 & 0.109 \end{bmatrix}$ kg.m^2.rad^{-2}	c	0.54 m
g	9.81 m.s^{-2}	d	0.40 m
A^P	1.16 m^2	ρ	1.225 kg.m^{-3}
V_P	6 m/s		

REFERENCES

[1] D. Carter, S. George, P. Hattis, and L. Singh, "Autonomous Guidance, Navigation, and Control of Large Parafoils," presented at the 18th AIAA Aerodynamic Decelerator Systems Technology Conference and Seminar, 2005.

[2] G. Strickert, "Study on the relative motion of parafoil-load-systems," *Aerospace Science and Technology,* vol. 8, pp. 479-488, 2004.

[3] G.-B. Hur, "Identification of Powered Parafoil Vehicle Dynamics from Modeling and Flight Test Data," Doctor of Philosophy Doctor of Philosophy, Texas A&M University, 2005.

[4] N. Slegers and M. Costello, "Model Predictive Control of a Parafoil and Payload System," *Journal of Guidance, Control and Dynamics,* vol. 28, 2005.

[5] J. R. Chambers, "Longitudinal Dynamic Modelling and Control of Powered Parachute Aircraft," Rochester Institute of Technology, 2007.

[6] P. Zipfel, *Modelling and Simulation of Aerospace Vehicle Dynamics*, 2 ed. 1801 Alexander Bell Drive, Reston, VA: American Institute of Aeronautics and Astronautics, 2007.

[7] N. Slegers and M. Costello, "Aspects of Control for a Parafoil and Payload System," *Journal of Guidance, Control and Dynamics,* vol. 26, 2003.

[8] V. Klein and E. Morelli, *Aircraft System Identification*. Reston, VA: AIAA, 2006.

[9] N. Nise, *Control Systems Engineering*, 6 ed. Danvers, MA: John Wiley & Sons, 2011.